EFFECT OF CHLORIDE IONS OF SALINE MEDIA ON CORROSION RATE OF CARBON STEEL IN SIMULATED CONCRETE SOLUTION

N.A. Khudhair[1], D.A. Challoob[2], M.K. Mohammed[1], A.J. Khaleel[2], M.F. Abbood[2], K.A. Abdulqader[3]

[1] *University of Baghdad, College of Sciences, Department of chemistry, Baghdad, Iraq*
noor.ali1105@sc.uobaghdad.edu.iq; mays.hasan@sc.uobaghdad.edu.iq
[2] *University of Naharain / College of Sciences / Department of chemistry / Baghdad / Iraq*
Dhuha.Abdulkareem@nahrainuniv.edu.iq; aeshah.Jamal@nahrainuniv.edu.iq; marwah.fawzi@nahrainuniv.edu.iq
[3] *University of Naharain / College of Pharmacy / Department of chemistry / Baghdad / Iraq.*
kany.azad@ced.nahrainuniv.edu.iq

Received 23.08.2024
Accepted 02.05.2025

Abstract :*In this study the corrosion behaviors of carbon steel (CS) in simulated concrete solution (KOH, NaOH, $Ca(OH)_2$) was investigated. Current density of corrosion (i_{corr}), potential of corrosion (E_a), anodic and cathodic Tafel slopes (β_a, β_c) were used to determine the resistance of polarization (Rp). The result indicated that the temperature increasing of the concrete electrolyte has slightly increased the rate of corrosion for the CS .This study also showed that the corrosion current of the polarized of CSRBs always increased linearly with chloride concentration in the rang 0.5 to 4.5% NaCl, the corrosion current are between 27 and 98 $x10^{-6}$ A/cm^2 for CS, these the corrosion rate values were not too high in comparison with the rates of the electrolyte free of chloride ions (25 - 62 $x10^{-6}$ A/cm^2).*

Keywords: *Chloride ions, Corrosion, Carbon steel, Platinum Auxiliary Electrode, Potentiostat.*
DOI: 10.65382/2221-8688-2026-1-21-30

Introduction

Corrosion is the deterioration or destruction and consequent loss of alloys or metals during electrochemical or chemical reaction with surrounding media [1]. Several factors affected on corrosion rate: moisture, temperature, atmospheric pollutants (chloride and sulfur), material type (different steel grade), techniques of protection, crevice presence and pollutants or stress [2]. Ex. iron rusting, the formation of green shells on copper vessels, etc.

Metallic Corrosion has two main groups:

- Wet corrosion: Liquids (electrolyte) is the corrosive media and an electrochemical corrosion process is undergone [3].
- Dry corrosion: Dry gas is the corrosive media; it's also called chemical corrosion [4, 5].

Metal dissolution during the oxidation process is considering an electrochemical corrosion. The chemical reactions of reduction and oxidation happened together and correlating. Corrosion occurs on oxidation reaction sites only. Electrochemical corrosion was caused by electrical current in which the electrons transferred among oxidation (loss of electrons) and reduction site (gain of electrons) [6, 7].

An important aspect of engineering component design is the selection of an appropriate surface engineering technology. The first step in modification technique of the surface is determined the substance and surface engineering supplies which include the following properties: erosion and corrosion resistance, wear resistance, pitting and fatigue resistance, thermal resistance etc. The different surface treatment, for the most part, used in engineering practice and presented as under. Surface engineering involves the enhancement of certain properties of the component surface separately from those of its bulk. The required improvements are related to surface corrosion and wear resistance and optical properties. The surface engineering processes of the component can be divided in to three essential groups [8, 9]:

1. The first group includes surface modifying without changing in the surface composition, ex. transformation hardening and surface re-melting.
2. The second group includes surface modifying with changing in the surface composition a critical feature of the process.
3. The third group includes coating processes of a suitable new material to the surface, such as: chemical vapor deposition (CVD) and electroplating processes [8].

Corrosion measurement is a practical quantitative method used to determine the corrosion current by immersing electrodes in a corrosive medium and continuously exposing them to this environment [10, 11].

In this research we studied the effect of NaCl different concentration (0.5, 2.5, 4.5%) on the corrosion rate of CS in simulated concrete solution at temperature range 0f (293-323K).

The Chemistry of Cement. Cement is a finely powdered powder that undergoes hydrolysis when combined with water, resulting in a chemical reaction. Hydration results in the formation of a highly durable and robust binding material for the aggregate particles. The choice of cement for a certain concrete or mortar will depend on the specific qualities needed. While there have been improvements in the synthesis of cement, the fundamental process has remained unchanged.

The cement raw materials mixture are:

1- Rocks of Calcareous ($CaCO_3$ > 75%, ex. chalk, marl and limestone,),

2- Rocks of Argillaceous ($CaCO_3$ < 40%, ex. shale and clay),

3- Rocks of Argillocalcareous (40-75% $CaCO_3$, ex. clayey limestone, clayey and marl). Cement contains over 90% of the oxides. Table (1) shows the composition of the oxide in the traditional cement [12].

Table 1. The oxide composition of traditional Portland cement [12]

Common name	Oxide	Abbreviation	Approximate composition Limits, (%)
Lime	CaO	C	60-66
Silica	SiO_2	S	19-25
Alumina	Al_2O_3	A	3-8
Iron oxide	Fe_2O_3	F	1-5
Magnesia	MgO	M	0-5
Alkalis			
soda	Na_2O	N	0.5-1
Potash	K_2O	K	0.5-1
Sulfur trioxide	SO_3	S	1-3

Four basic factors described the cement's physical properties.

1. *The fineness*. On the cement particles surface, a chemical reaction has been started between water and cement. That means the hydration increases with increasing cement surface area. Therefore, the fine cement will improve strength and develop heat more rapidly than coarse cement [13-15].

2. *The hydration*. The hydration process is water and cement chemical combination to produce a very strong and hard binding media for particle aggregation in concrete. Heat is evolved at the hydration process end, and it is defined as Cal/gm. In typical construction cases when structural members are not very big, heat dissipation is no problem. In the context of the concreting in the cold weather, this heat is beneficial. However, at high temperatures and during the construction of large concrete structures, this heat produced might lead to the formation of thermal cracks, which must be prevented. The process of hydration of cement can be measured by quantifying $Ca(OH)_2$ content in the dough and measuring the heat generated during hydration. On the other hand, there are other important parameters that are important, including the quantity of anhydrate paste of cement, anhydrate cement paste specific gravity, and the quantity of chemically combined water [16-20].

3. *The strength.* The most significant cement property is the hardened strength. The rate of cement solidification is influenced by the

physical and chemical characteristics of the cement, the conditions in which it is cured, and the amount of water to cement [21].

4. *The soundness.* Soundness is a characteristic of cement paste that refers to its capacity to maintain its volume once it has finished setting. The lack of soundness is caused by the existence of unbound CaO and unbound MgO in cement. The hydration of these components occurs at a slower rate following the cement's solidification. Expansion occurs because $Mg(OH)_2$ and $Ca(OH)_2$ have a higher volume [22].

Experimental part

Material and Methods. The experimental work consisted of the following three stages:

1) Surface Preparation. Carbon steel samples were cleaned by immersing them in concentrated hydrochloric acid (HCl) to remove surface oxides and impurities. After acid treatment, the samples were rinsed thoroughly with distilled water. Subsequently, they were prepared for placement in the experimental setup.
2) Electrochemical Setup. A carbon steel specimen with a surface area of 1 cm^2 was mounted as the working electrode and positioned in the electrochemical testing apparatus. The test solution used was a blank simulated pore solution, composed of sodium hydroxide (NaOH, 8 mg), potassium hydroxide (KOH, 22.44 mg), and calcium hydroxide ($Ca(OH)_2$, 2g) dissolved in 1 liter of distilled water, replicating the chemical environment of concrete.

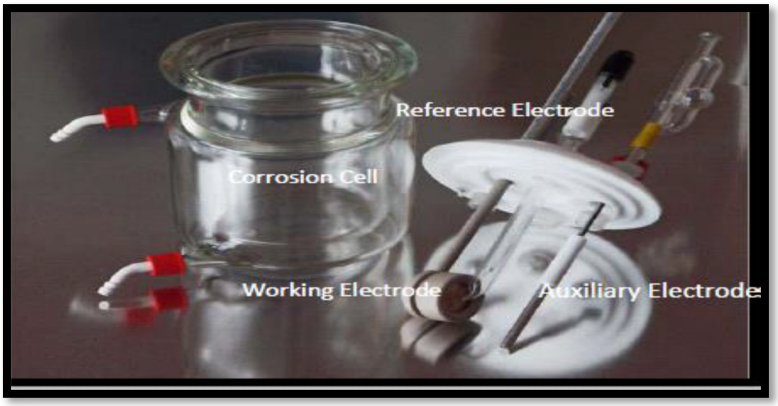

Fig. 1. Electrochemical cell of corrosion consists of three electrodes

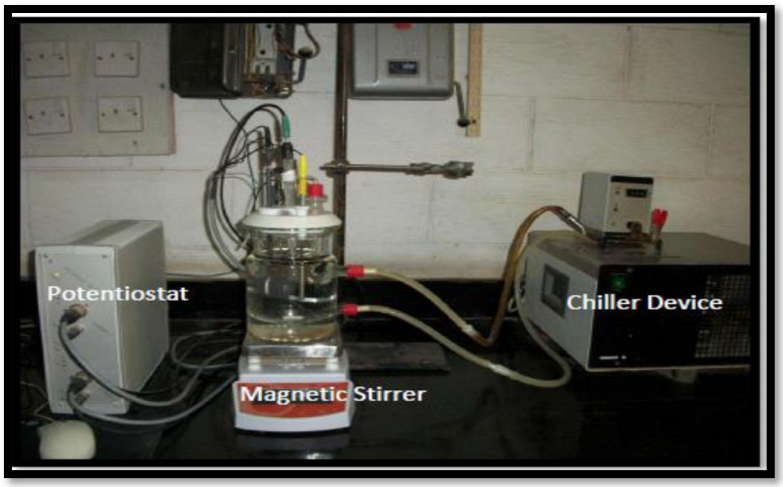

Fig. 2. Modern electrochemical system.

3) Addition of Chloride Ions. To investigate the effect of chloride concentration, NaCl was added to the blank solution at three different concentrations: 0.5%, 2.5%, and 4.5% by

weight. For each concentration, a separate carbon steel sample—cleaned using the same procedure described in step 1—was used in the corrosion testing.

Electrochemical system. The electrochemical system used for electropolymerization and corrosion measurements consists of three main components: a potentiostat, an electrochemical cell, and electrodes (Fig.s 1 and 2).

Potentiostat. Electrochemical experiments were performed using a potentiostat manufactured by WENKING M Lab, Bank Elektronik-Intelligent Controls GmbH. The M Lab system is a multichannel potentiostat/galvanostat that interfaces with a computer via an RS-232 cable. It includes a hardware control board and supports three operational modes for each channel:

- **Galvanostatic mode** (constant current),
- **Potentiostatic mode** (constant potential),
- **Open-circuit mode** (no imposed current or voltage).

These modes allow precise control and monitoring of the electrochemical processes involved in both electropolymerization and corrosion testing.

Cell. The Pyrex cell has a capacity of 1 liter and consists of two vessels, an exterior and an internal one.

Electrodes. The potential of the working electrode is determined vs. the reference electrode. It is important to keep the gradient of ohmic resistance reduced, and the flows of the electrical current are between the working electrode and the auxiliary electrode. The composition of the cell constituents and its assignment are expressed below.

Platinum Auxiliary Electrode. The auxiliary electrode used in this study was made of high-purity platinum. Due to its excellent catalytic activity and high corrosion resistance, platinum is ideal for serving as an auxiliary (counter) electrode. Its primary function is to complete the electrical circuit by carrying the current to or from the working electrode during electrochemical measurements.

Reference Electrodes. The working electrode potential is determined based on the potential of the reference electrode. The potential of the reference electrodes is widely recognized and specific, measuring 0.244V at a temperature of 25°C, this electrode has two tubes; the outer one consists of the media of corrosion. The inner one consisting of Hg/ Hg_2Cl_2, KCl. The distance between the working electrode and reference electrode must be 2 mm.

The potential of the working electrode is measured relative to a reference electrode with a well-defined and stable potential. In this study, a saturated calomel electrode (SCE) was used, which has a standard potential of +0.244 V versus the standard hydrogen electrode (SHE) at 25°C. The reference electrode consists of two concentric tubes: the outer tube contains the corrosion medium, while the inner tube is filled with a mercury/mercurous chloride (Hg/Hg_2Cl_2) system in saturated potassium chloride (KCl) solution.

For accurate measurements, the distance between the working and reference electrodes was maintained at 2 mm to minimize potential drop (iR drop) in the electrolyte.

Working Electrode. The working electrode used in this study was a circular flat specimen with a diameter of 2.5 cm, mounted in a disk-fix electrode holder designed for planar samples. The specimen was positioned between an electrically conductive brass backing plate and a masking cover with a defined aperture, exposing a specific surface area to the electrolyte—typically 1 cm^2, which is preferred for standardized testing. To prevent leakage and ensure the specimen remains dry on the non-exposed side, a washer was employed to seal the interior of the disk-fix holder. Prior to polarization testing, the electrode was immersed in the electrolyte for a fixed period to allow stabilization of the electrochemical interface. This stabilization step is critical for obtaining reliable and reproducible corrosion measurements.

Chiller. To maintain a constant and controlled temperature during the experiment, the solution circulating through the external vessel was cooled using a chiller device. This ensured thermal stability throughout the electrochemical measurements.

Magnetic Stirrer. A magnetic stirrer was employed to ensure uniform mixing of the electrolyte solution. It operates by generating a rotating magnetic field that drives a stir bar placed within the solution. During the

experiments, the stirring speed was maintained between 300 and 600 revolutions per minute (rpm) to ensure consistent distribution of ions and prevent concentration gradients.

Results and discussion

The results of this work study the corrosion behaviors of carbon steel (CS) in simulated concrete solution (KOH, NaOH, $Ca(OH)_2$) and study the effect of chloride ions at increasing temperatures up to 323 K, using the Tafel extrapolation procedure.

Corrosion Behavior of Carbon Steel in Simulated Concrete Solution. The electrochemical corrosion kinetics of carbon steel (CS) in simulated concrete pore solutions were evaluated using Tafel polarization curves (potential **E** vs. logarithm of current density **i**). Key parameters extracted from the Tafel plots include the corrosion potential ($\mathbf{E_{corr}}$), anodic and cathodic Tafel slopes ($\boldsymbol{\beta_a}$ and $\boldsymbol{\beta_c}$, respectively), and the corrosion current density ($\mathbf{i_{corr}}$). These values were used to calculate the polarization resistance ($\mathbf{R_p}$) of the system.

The corrosion rate was subsequently converted into Faradaic corrosion rate units (mm/year) using standard electrochemical equations [23].

The corrosion rate measurements for carbon steel (CS) showed relatively low values under the tested conditions (see Tafel plots in Fig. 3 [24]). However, a slight increase in the corrosion rate was observed with increasing temperature of the simulated concrete electrolyte, indicating the temperature dependence of the corrosion process. This trend is clearly demonstrated in Table 2.

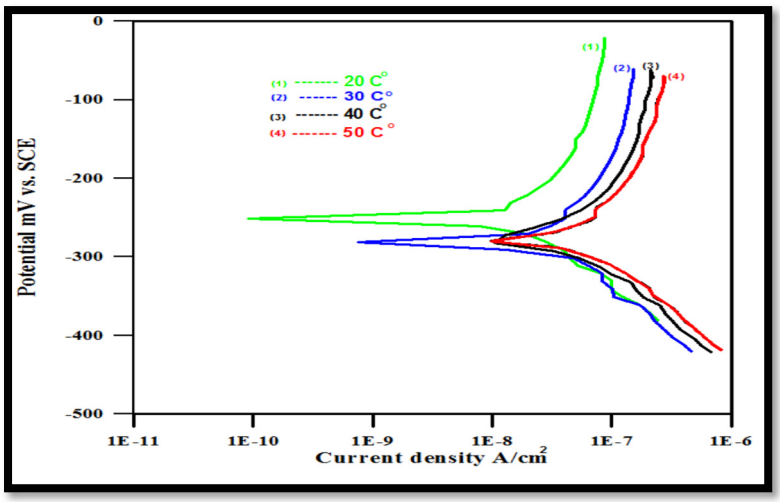

Fig. 3. Tafel plots of CS in simulated concrete solution at 293, 303, 313, and 323 K

Table 2. Corrosion rate parameters of CS in simulated concrete solution at 293, 303, 313, and 323 K

Sample	T(K)	E_{corr} (mV)	i_{corr} ($*10^{-6}$ A/cm^2)	ßc (mV/Dec)	ßa (mV/Dec)	R_p (Ω.cm^2)	CR(WL) g.m^{-2}d^{-1}	CR(PL) mmpy
0%NaCl	293	-341	25.7	-122.6	138.3	1158.493	7.25	1.481
	303	-380.3	32.97	-130.2	178	1032.11	9.07	1.565
	313	-421.8	40.54	-90.6	167.8	650.177	10.96	1.653
	323	-393.9	62.95	-83.5	187.6	405.982	16.6	1.913

**CR(WL) corrosion rate as weight loss,*
***CR(PL) corrosion rate as penetration loss*

The slopes of the anodic and cathodic branches of the Tafel polarization curves were used to determine the anodic (β_a) and cathodic (β_c) Tafel slopes, as presented in Table 2. These values reflect the electrochemical kinetics of the corrosion process and indicate that the system exhibits quasi-reversible behavior.

The corrosion current density (i_{corr}) of carbon steel was found to be higher at 323 K compared to 293 K, suggesting an acceleration of

the corrosion process with increasing temperature. This difference is attributed to variations in the calculated polarization resistance (Rp). The measurement of Rp shares similar methodological requirements with full Tafel analysis but offers a faster means of assessing corrosion activity. It is particularly useful for detecting corrosion upsets and implementing timely corrective actions [25, 26].

The effect of chloride ions on Corrosion behavior of CS. The effect of chloride ion content in the artificial concrete solution on the corrosion behavior of CS was studied using chloride concentration at a range of 0.5% to 4.5% weight percent, and the effect of rising electrolyte temperature was also followed at a range of 293 to 323 K.

Fig.s 4, 5, and 6 represented Tafel plots of CS in chloride-containing concrete solutions at different temperatures, respectively.

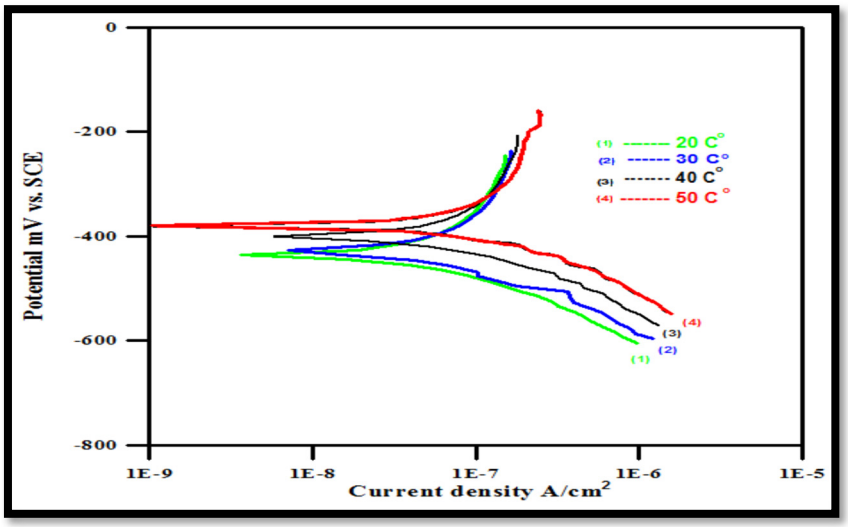

Fig. 4. Tafel plots of CS in chloride-containing simulated concrete solution (0.5% NaCl) at 293, 303, 313, and 323 K

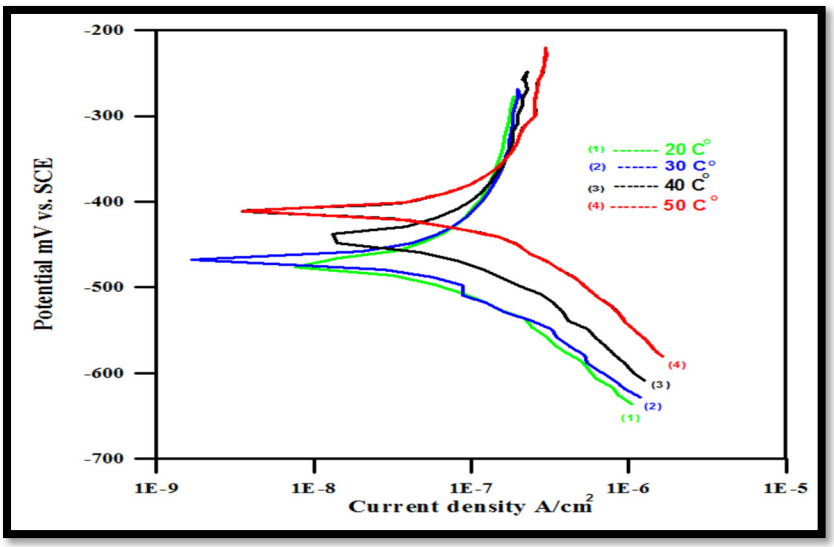

Fig. 5. Tafel plots of CS in chloride containing simulated concrete solution (2.5% NaCl) at 293, 303, 313, and 323 K

The data in Tables 3 showed that the corrosion current of the polarized CSRBs always increased linearly with chloride concentration in the range of 0.5 to 4.5% NaCl; the corrosion currents are between 27 and 98 x 10^{-6} A/cm^2 for CS. These corrosion rate values were not too high in comparison with the rates of the electrolyte free of chloride ions (25 - 62 x10^{-6} A/cm^2), as shown previously in Table 2.

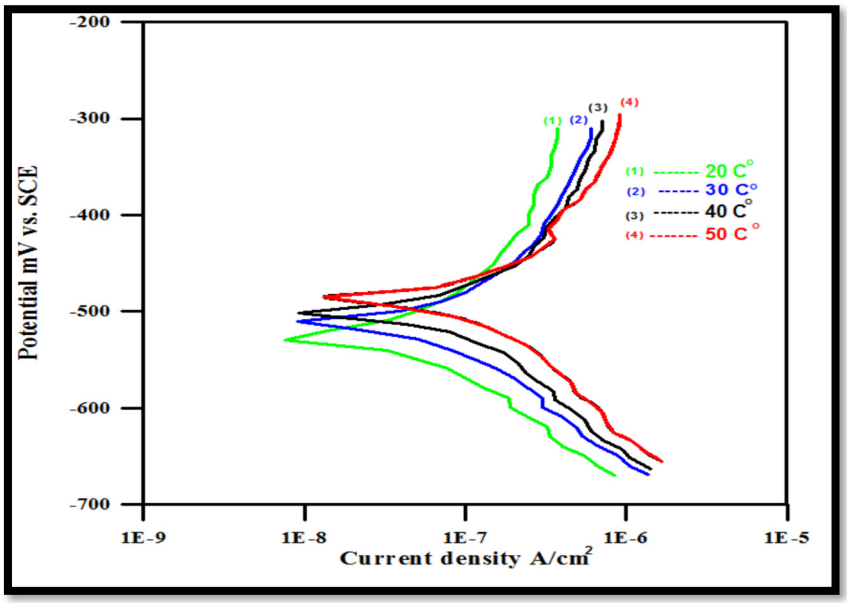

Fig. 6. Tafel plots of CS in chloride-containing simulated concrete solution (4.5% NaCl) at 293, 303, 313, and 323 K.

Table 3. Corrosion rate parameters of CS in simulated concrete solution containing chloride ions at 293, 303, 313 and 323 K.

NaCl %	T(K)	E_{corr} (mV)	i_{corr} (*10^{-6} A/cm^2)	ß$_c$ (mV/Dec)	ß$_a$ (mV/Dec)	R_p (Ω.cm^2)	CR(WL) g.m^{-2}d^{-1}	CR(PL) mmpy
0.5	293	-440.2	27.66	-82.9	147.4	673.89	5.41	0.324
	303	-432.5	35.3	-97.1	159.5	967.41	7.32	0.413
	313	-397.2	45.4	-104.3	171.7	1323.1	9.8	0.53
	323	-372	69.67	-115.9	215.5	2324.34	15.9	0.812
2.5	293	-475.5	40.35	-96.4	170	1118.79	8.6	0.472
	303	-474	43.1	-103.7	173.9	1259.97	9.3	0.503
	313	-435.4	71.48	-137.9	226	2714.73	16.4	0.833
	323	-411.9	76.24	-105.7	185.9	2268.14	17.6	0.888
4.5	293	-538.2	53.12	-117.1	196.1	1740.42	11.8	0.62
	303	-512.7	67.61	-133.4	137	2039.65	15.4	8079.98
	313	-509.4	95.65	-144	176	3347.16	22.4	1.11
	323	-499.2	98.38	-115	155.7	2867.29	23.1	1.15

The indicated R_p decreased as the concentration of NaCl increased, providing strong evidence that nonconductive oxide rust products, rather than chlorides, formed on the surface of the CSRB [27-29].

The electrodeposited layers were examined by AFM; the surface morphology of a protective coated layer plays a great role in enhancing the corrosion protection efficiency. More uniform compacted grains may lead to more inhibition results. 3D views of AFM images for all applied layers were estimated in addition to the statistical determination of the particle size distribution figures. The AFM images with 3D views clarify the surface roughness and morphology views [30] (Fig. 7).

The obtained values from the polarization experiments are supported by the rising dark area in the optical images above with the NaCl [31].

As the concentration rises, the 3D view morphology inferred from AFM analysis shows increasing attack of chloride ions [32] (Fig. 7).

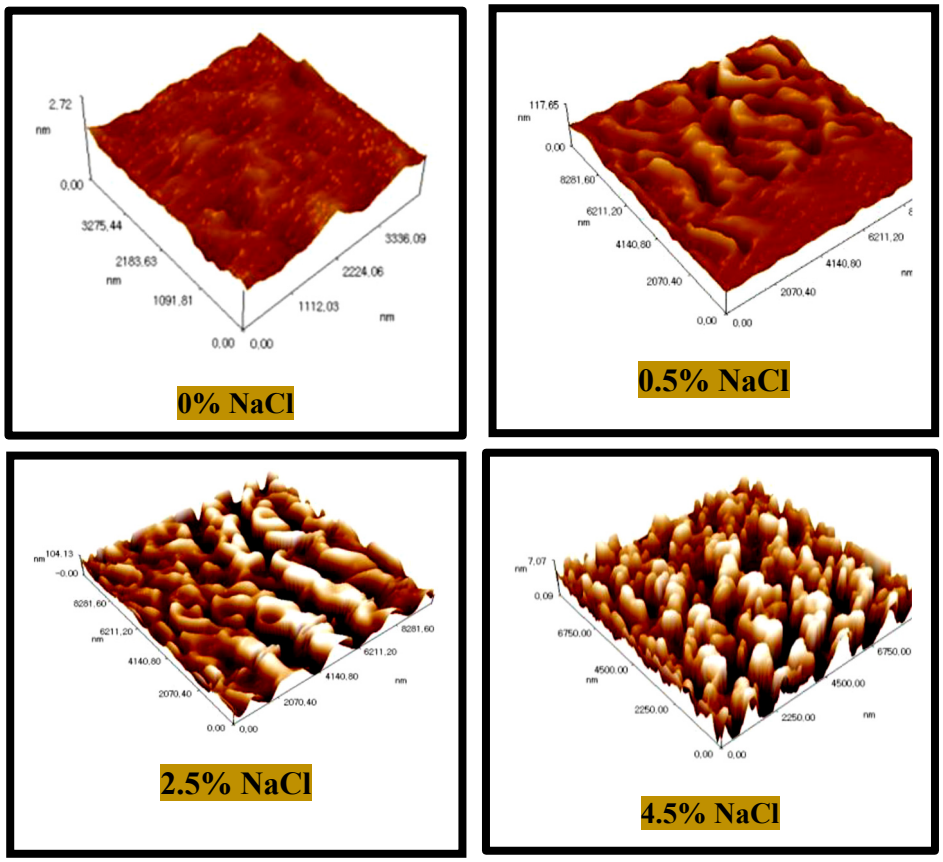

Fig. 7. AFM images in three dimensions showing the polarization of CSRB in an artificial concrete solution with varying NaCl concentrations

Conclusion

The following conclusions can be drawn from this investigation: Atomic force microscopy (AFM) analysis strongly corroborated the findings obtained from the Tafel polarization plots. The corrosion rates of carbon steel rebars (CSRB) increased with rising NaCl concentration within the range of 0.5% to 4.5%. Furthermore, the corrosion rates also exhibited an increasing trend with elevated temperatures in the simulated concrete solution.

References

1. Zaki A. *Principles of corrosion engineering and corrosion control*; 1st ed. Elsevier. 2006. 656 p. DOI: 10.1016/B978-0-7506-5924-6.X5000-4
2. Luigi D., Armin M., George K., The effect of atmospheric corrosion on steel structures: A state of the art and case study. *Buildings*, 2021, **Vol. 11**, 571. DOI: 10.3390/buildings11120571
3. Makhlouf A.S.H. *Handbook of Smart Coatings for Materials Protection.* Elsevier Science, 2014. 628 p.
4. Frame Project Team, *A Guide To Corrosion Protection*; Cracking Down on Corrosion, American Iron and Steel Institute, 2000 Town Center, Suite 320, Southfield, 1999.
5. Einar B. *Corrosion and protection–engineering materials and processes*. Springer-Verlag London Limited. 2004. 5 p.
6. Norio S. *Basics of corrosion chemistry*. Wiley-VCH Verlag GmbH & Co. KGaA. 2011. 1 p.
7. Mohammad H. Modeling of pipeline corrosion control by cathodic protection. Ph.D. Thesis, Department of Production Engineering and Metallurgy, University of Technology, Iraq, 2006.

8. Mellor B. *Surface coatings for protection against wear*. Woodhead publishing limited: Cambridge England. 2006.
9. Tadeusz B., Tadeusz W. *Surface engineering of metals principles, equipment, technologies*. CRC Press. 1998. 1-3 p.
10. Metal Samples Company "Introduction to Corrosion Monitoring", Discovered Available online: http://www.alspi.com/corrosion-intro.
11. Lietai Y. *Techniques for corrosion monitoring*. Woodhead Publishing Limited. 2008. 2 p.
12. Brunauer S., Copeland L., The chemistry of concrete. *Scientific American*. 1964, **Vol. 210(4)**, p. 80-93.
13. Ehikhuenmen S., Igbal U., Balogunl O., Oyebisi S. The influence of cement fineness on the structural characteristics of normal concrete. *IOP Conference Series: Materials Science and Engineering*. 2019, **Vol. 640**ç DOI: 10.1088/1757-899X/640/1/012043.
14. Bharadwaj N., Nayak A. *Manual on concrete laboratory*. Burla: Department of Civil Engineering, Veer Surendra Sai University of Technology. 1 p.
15. Ali M., Arif E., Burak F., Kambiz R., Effect of cement fineness on properties of cementitious materials containing high range water reducing admixture. *Journal of Green Building*. 2017, **Vol. 12(1)**, p. 142-167. DOI: 10.3992/1552-6100.12.1.142.
16. Carmona J., Garcés P., Climent M., Efficiency of a conductive cement-based anodic system for the application of cathodic protection, Cathodic prevention and electrochemical chloride extraction to control corrosion in reinforced concrete structures. *Corrosion Science*. 2015, **Vol. 96**, p. 102-111. DOI: 10.1016/j.corsci.2015.04.012.
17. Jiong H., Zhi G., Kejin W. Influence of cement fineness and water-to-cement ratio on mortar early-age heat of hydration and set times. *Construction and Building Materials*. 2014, **Vol. 50**, p. 657-663. DOI: 10.1016/j.conbuildmat.2013.10.011.
18. Abdel Rahim M. *The effect of admixtures on concrete properties.* M.Sc thesis, University of Khartoum, Faculty of Engineering Department, 3 p.
19. Steven H., Kosmatka Beatrix K., William C. *Design and control of concrete mixtures*. Portland Cement Association. 2002. 4 p.
20. Gupta O. *Element of Chemical Process Technology.* Khanna Publishing House - Technology & Engineering. 2018. 319 p.
21. Metwally A., Compressive strength prediction of Portland cement concrete with age using a new model. *Housing and Building National Research Center*. 2014, **Vol. 10(2)**, p. 145-155. DOI: 10.1016/j.hbrcj.2013.09.005.
22. Kabira H., Hootona R., Popoffb N. Evaluation of cement soundness using the ASTM C151 autoclave expansion. *Cement and Concrete Research*. 2020, **Vol**. **136**, p. 1-16. DOI: 10.1016/j.cemconres.2020.106159.
23. Fletcher S. Tafel slopes from first principles. *Journal of Solid State Electrochemistry*. 2009, **Vol. 13**, p. 537-549. DOI: 10.1007/S10008-008-0670-8.
24. Liu X., Niu D., Li X., Lv Y., Fu Q. Pore solution pH for the corrosion initiation of rebars embedded in concrete under a long-term natural carbonation reaction. *Applied Sciences*. 2018, **Vol. 8(1)**, p. 128. DOI: 10.3390/app8010128.
25. Cho J., Schaab S., Roether J., Boccaccini A. Nanostructured carbon nanotube/TiO_2 composite coatings using electrophoretic deposition (EPD). *Journal of Nanoparticle Research*. 2008, **Vol**. **10(1)**, p. 99-105. DOI: 10.1007/s11051-007-9230-x.
26. Haider A. Study the effect of punica granatum as oral antifungal on the corrosion inhibition of dental amalgam alloy in saliva. *Journal of Materials and Environmental Sciences*. 2018, **Vol**. **9(2)**, p. 662-671. DOI: 10.26872/jmes.2018.9.2.73.
27. Osial M., Wiliński D. Organic substances as corrosion inhibitors for steel in concrete–an overview. *Journal of Building Chemistry*. 2016, **Vol**. **1**, p. 43-53. DOI: 10.17461/j.buildchem.2016.107.
28. Serdar M., Stipanović O., Bjegović D. Primjena nehrđajućih čelika kao armature u betonu. *Građevinar*. 2010, **Vol. 62(3)**, p. 219-227.
29. Chauhan A., Sharma U. Influence of temperature and relative humidity variations on non-uniform corrosion of reinforced concrete in structures. *Structures*. 2019, **Vol.**

19, p. 296-308. DOI: doi.org/10.1016/j.istruc.2019.01.016.
30. Khudhair N., Ali T., Mayasa I., Marwah H. Synthesis, identification and experimental studies for carbon steel corrosion in hydrochloric acid solution for polyimide derivatives. *In AIP Conference Proceedings*. 2020, **Vol. 2290**. DOI: 10.1063/5.0027443.
31. Khudhair N., Al-Sammarraie A., Investigation on the effect of origin of carbon steel reinforcing bar on the corrosion behavior in artificial concrete solution. *Journal of Global Pharma Technology*. 2019, **Vol. 11(5)**, p. 76-81.
32. Khudhair N., Kadhim M., Khadom A. Effect of trimethoprim drug dose on corrosion behavior of stainless steel in simulated human body environment: experimental and theoretical investigations. *Journal of Bio- and Tribo-Corrosion*. 2021, **Vol. 7(124)**, 124. DOI: 10.1007/s40735-021-00559-8.